NRC BELL 412 AIRCRAFT FUSELAGE PRESSURE AND ROTOR STATE DATA COLLECTION FLIGHT TEST

Arthur Gubbels, Stephan Carignan, Kristopher Ellis, Jeremy Dillon, Matthew Bastian, Carl Swail[1], and Colin Wilkinson[2]

[1] National Research Council of Canada, Flight Research Laboratory
Bldg U-61, Ottawa, Ontario, Canada, K1A 0R6
e-mail: bill.gubbels@nrc.ca

[2] General Dynamics Information Technology
44421 Airport Road, California, Maryland, USA, 20619
e-mail: colin.wilkinson@gdit.com

Key words: static pressure, air wake, computational fluid dynamics, flight test data, helicopter

Abstract: The Flight Research Laboratory (FRL), of the National Research Council of Canada owns and operates a Bell 412 research helicopter that is essentially the same type aircraft as the Canadian Department of National Defense (DND) Griffon. DND has a major research thrust involving the improvement of aerodynamic and simulation models of this aircraft. In collaboration with DND, FRL has recently performed flight testing of the Bell 412 in support of this effort. In addition to the already extensive suite of inertial and engine data collected on a regular basis, the aircraft was instrumented with 256 static pressure transducers located at various positions around the fuselage, engine cowls and tail boom. Rotor flapping, lead-lag and strain quantities were also instrumented. Data was acquired in many different flight regimes throughout the aircraft envelope, including hover, cruise flight, climbs and descents and autorotation. Data was also collected in the hover both in front of a hangar face and in a field clear of obstacles in two different wind conditions, with a set of ground based anemometers to collect air wake data. This extensive data set is intended to serve as validation data for computational fluid dynamics (CFD) models of the aircraft and to extend the knowledge base of the characteristics of airflow around a helicopter in flight. The data will also allow a better understanding of the effects of buildings on the air wake of a helicopter, an important consideration for ship dynamic interface. This paper describes the instrumentation set up, flight testing conducted and provides samples of the flow field data collected.

Figure 1: Bell 412 Advanced Systems Research Aircraft

1 INTRODUCTION

The flow field around a rotorcraft is extremely difficult to model. There is an overwhelming set of aerodynamic challenges, which render numerical simulation almost impossible. The most complex issue involves the computation of the unsteady 3D rotor wake, which not only has to contend with intractable interference issues with the fuselage, tail boom and tail rotor but has its own origins in equally complicated separated flows and blade vortex interactions. Other traditional aerodynamic problems associated with bluff body separations coupled with other noise and vibration issues, has made the rotor flow field simulation a daunting task for researchers.

To date, no full scale data exists of the flow field around a helicopter in-flight. Collection of surface pressure measurements distributed around the helicopter to use as validation data would enable researchers to advance the state-of-the-art in CFD code.

Improvements in the prediction of turbulent and unsteady flow will have a far reaching impact. For instance, although CFD has been used for years to predict lift, it has not been able to accurately characterize drag. Helicopter manufacturers are plagued by an inability to correctly position vertical and horizontal stabilizer and have to resort to time consuming and costly flight trials to compromise between loads and handling qualities.

This report describes the instrumentation installed in the NRC Bell 412 (Figure 1) and the flight testing conducted to acquire a data set sufficient for comparison with current and future CFD models of the Bell 412 in various flight conditions. Data was also collected in the hover both in front of a hangar face and in a field clear of obstacles with a set of ground based anemometers used to collect air wake data. This data will allow a better understanding of the effects of buildings or hangars on the air wake of a helicopter, an important consideration for ship dynamic interface and this air wake data will also be used for the validation of CFD models.

2 TEST AIRCRAFT AND INSTRUMENTATION

The Advanced Systems Research Aircraft (ASRA) is a Bell 412HP, that is operated by the NRC in the experimental category. It is a twin engine medium helicopter with a maximum gross weight of 11,900 pounds (5410 kilograms). Project test flights for pressure data collection utilized the standard mechanical flight control system. Installed in the aircraft is an experimental fly-by-wire system and data recording system. This VME based data acquisition system records a large selection of parameters to removable hard disk at 128 Hz.

Control Positions. All of the aircraft control positions are measured using potentiometers and recorded via the data acquisition system. The recorded parameters include: the safety pilot's cyclic, pedal, collective and throttles, as well as the swash plate position and tail rotor actuator position.

Air Data Measurement. A nose boom is attached to the aircraft to enable accurate measurements of angle of attack and sideslip, using vanes; and static and total pressure, using a directional probe. Both the vanes and the directional probe are positioned well ahead of the aircraft and out of the rotor downwash while in forward flight. The boom protrudes from the fuselage by approximately 7.5 ft, and is made of a carbon fibre composite for high stiffness. Pressure transducers, installed in the forward avionics bay, acquire the pressure data.

GPS. A NovAtel GPS is installed in the Bell 412 ASRA to provide a high degree of position and velocity accuracy. The unit can operate in differential mode using a real time link to a differential GPS ground station, to achieve sub-meter level accuracy. The GPS receiver antenna is located above the cabin to limit line of sight obstructions between the aircraft and the satellites during manoeuvring.

Inertial Data. A Litton 92 Inertial Reference System and Honeywell HG1700 IMU, Kalman filtered with GPS, both provide aircraft accelerations, rates and attitudes. These units can also provide ground speed and position information.

Radar and Laser Altimeters. A commercially available aircraft radar altimeter is installed in the helicopter to provide a measure of height above ground. A laser altimeter is also installed in the aircraft to provide a more accurate measure of height above ground when working in the 0-300 ft (0-100 meters) AGL regime.

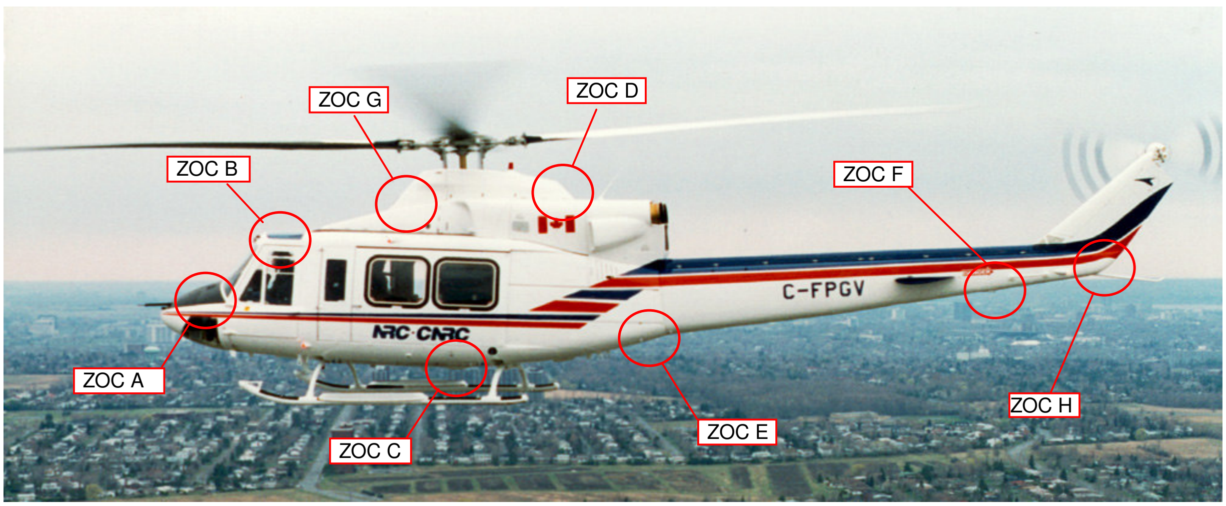

Figure 2: ZOC locations

Pressure Sensing. A fuselage pressure sensing system was installed for this flight test, consisting of 256 static ports located at various positions around the aircraft. These ports were contained in a button shaped package roughly the size of a small coin, and were mounted on the fuselage of the aircraft so that they protruded very little above the surface. Each button was connected to a ZOC23B module, produced by Scanivalve Corp., using a tubing with an inner diameter of 0.06 inches. The ZOC (Zero, Operate and Calibrate) module can acquire pressure from 32 buttons, and there were 8 ZOCs located in various locations around the aircraft, as shown in Figure 2. The ZOC modules were bench calibrated prior to installation on the aircraft. Each ZOC module was bonded to an appropriate aircraft surface using double sided foam tape. Each pressure button was bonded to the fuselage using double sided 1/2 mil polyester film with acrylic adhesive. Foil Tape was used over all exterior tubing runs to ensure it was firmly adhered to the aircraft fuselage. Constant tubing length was required to allow dynamic pressure measurements. The tubing length from each button to each ZOC was kept constant at 2 meters. The use of this constant tubing length necessitated the coiling of some of the tubing at the ZOC location as some buttons were located closer to the ZOC than others. A sample pressure button installation is shown in Figure 3. Given the relative size of the transducers and tubing, it was not expected that the handling qualities of the aircraft would be affected. Frequent inspections of the transducers and tubing were conducted during the flight testing to ensure the integrity of the installation. The aircraft was restricted to Day VFR flight only with no precipitation and at temperatures above 5º C, since the operating temperature range of the ZOCs prevented their use below 0º C, and precipitation could block the tubing preventing accurate readings.

Figure 3: Typical pressure button installation

The pressure data acquisition system used sensors made by Scanivalve Corp and consists of a DSM 3000 interface control unit and eight 32 channel ZOC modules. The ZOC modules allow sequential scanning of the 32 pressure taps. The DSM 3000 contains 9 analog to digital convertors, 8 to measure pressure inputs and one to measure temperature inputs. The DSM (Digital Service Module) scans each pressure port on the ZOC, applies a temperature correction and then transmits the data to the aircraft project data system for storage. The ZOC's require a set of pneumatic lines for control of the three operating modes and provision of calibration, purge and reference pressures. A schematic of the ZOC pressure control system is shown in Figure 5. Control pressure was provided from an onboard 1800 psi nitrogen pressure bottle and was regulated to 65 psi. The DSM was configured to electrically operate three pneumatic valves so that commands from the DSM could be used to apply the correct pressure to the correct control lines. The DSM and control pressure system was installed in a rack located in the aircraft cabin, as shown in Figure 4. The pressure in the bottle, control and purge lines were monitored via 3 separate pressure gauges. In order to clear the pressure taps, a PURGE command was used. This allowed low-pressure nitrogen at 2 psi to flow out from the ZOC control head to the taps to clear moisture and debris from the lines. As was the case with each of the pressure lines, the length of the reference line to each ZOC had to be kept constant so that as the reference changed dynamically, it would have an equal effect on each ZOC reading. Each of these reference lines were sourced from a reference block, with the source pressure coming from the project static system on the aircraft. Operation of the DSM was done through a Telnet window from the on-board PC workstation. Periodically, a zero calibration (CALZ) was performed to ensure that the pressure readings were stable and of high quality.

For the tests carried out on the aircraft, the DSM was set up to continuously scan all the pressure channels and send binary data in UDP packets via Ethernet to the main aircraft project data system. The pressure data was then recorded as a separate data record synchronized with data from other data sources on the aircraft. The scan rate was set such that a complete scan of all 256 channels was completed in about 15 ms.

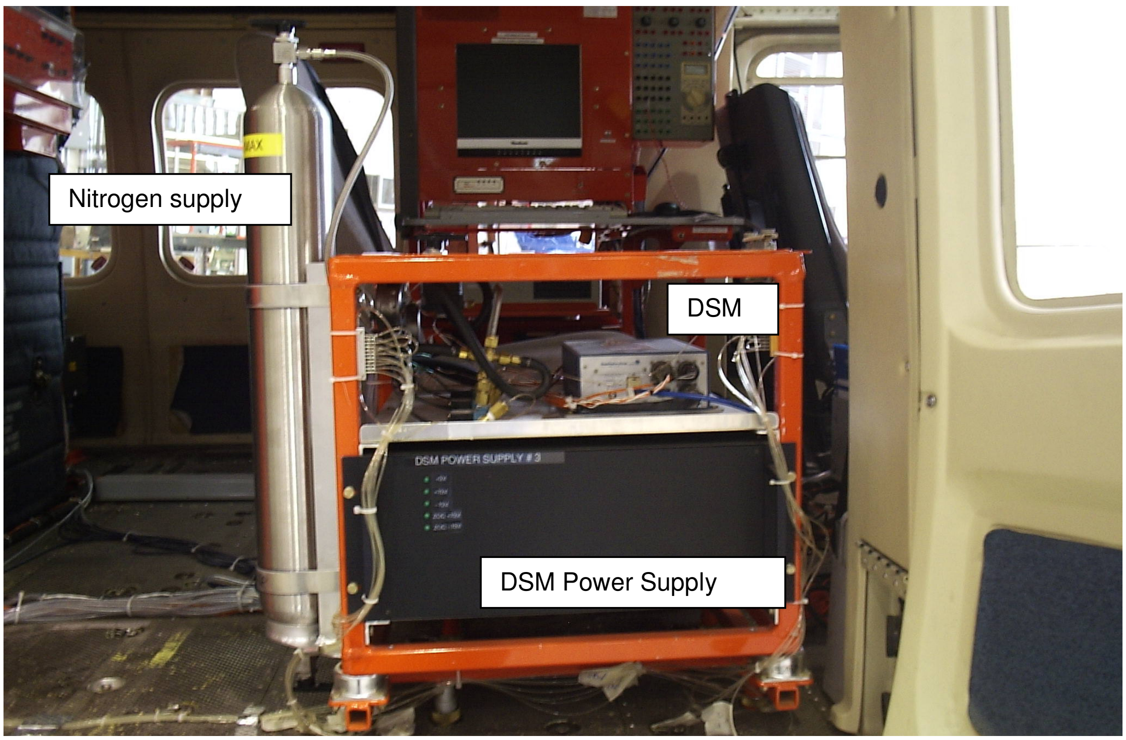

Figure 4: IMS Rack installation in cabin behind pilot

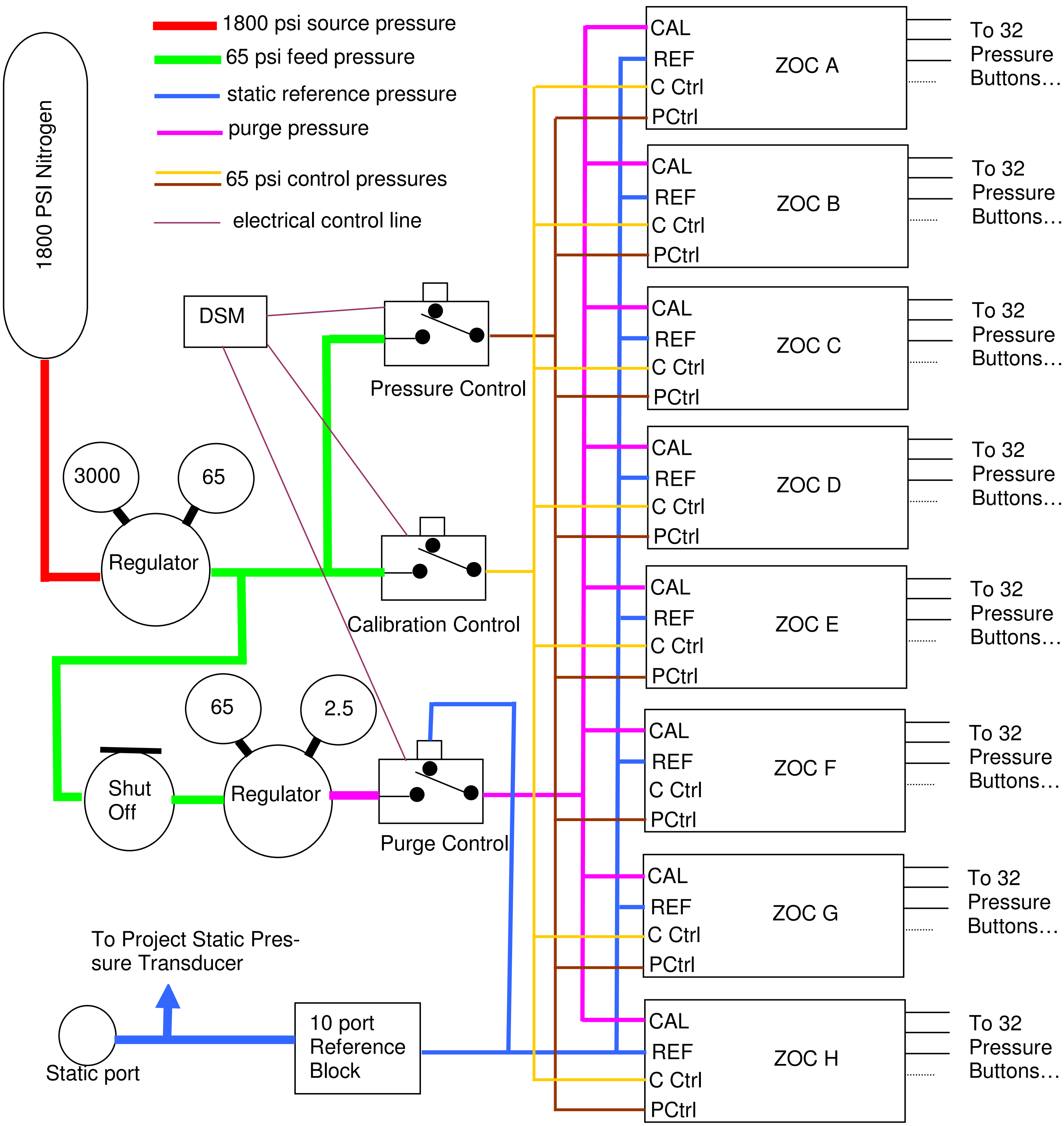

Figure 5: Schematic of ZOC pressure control system

Engine/Main Rotor Data. Engine parameters, including fuel flow, compressor and power turbine speed, mast torque, and main rotor rpm were recorded at 64 Hz. In addition, rotor flapping, lead-lag and blade strain data was acquired using a mast mounted data acquisition and transmitter unit. A commercial telemetry system for rotating applications, a KMT CT-16 Rotate, was used to signal condition the data on the rotor head and transmit it to a fuselage mounted receiver. The KMT CT-16 Rotate (Figure 6) collected 4 channels of flapping data, 4 channels of lead lag data and 4 channels of blade strain data and transmitted this data to a receiver unit in the aircraft fuselage at a data rate of 1633 Hz. A single board computer processed the data and re-transmitted it to the aircraft project data system at 400 Hz for data recording. An instrumented blade loaned by the Aerospace Engineering Test Establishment, part of the Canadian DND, was installed on the aircraft. The strain gauges on this blade (Figure 7) measured blade flap-wise and cord-wise bending at stations 132 (Figure 8) and 36. Further details regarding the standard instrumentation installed on the NRC Bell 412 ASRA are available in references 1, 2 and 3.

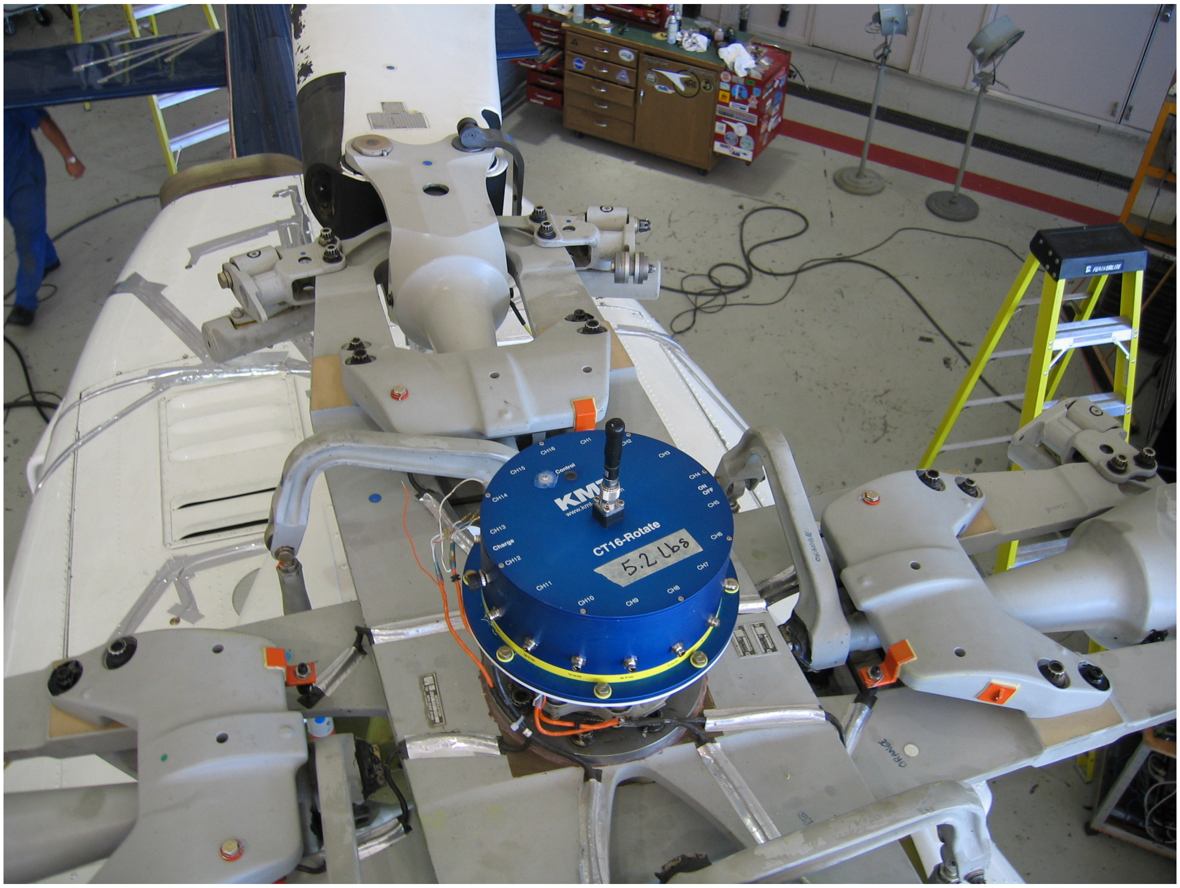

Figure 6: KMT CT-16 Rotate data acquisition unit and transmitter

Figure 7: Instrumented Bell 412 main rotor blade

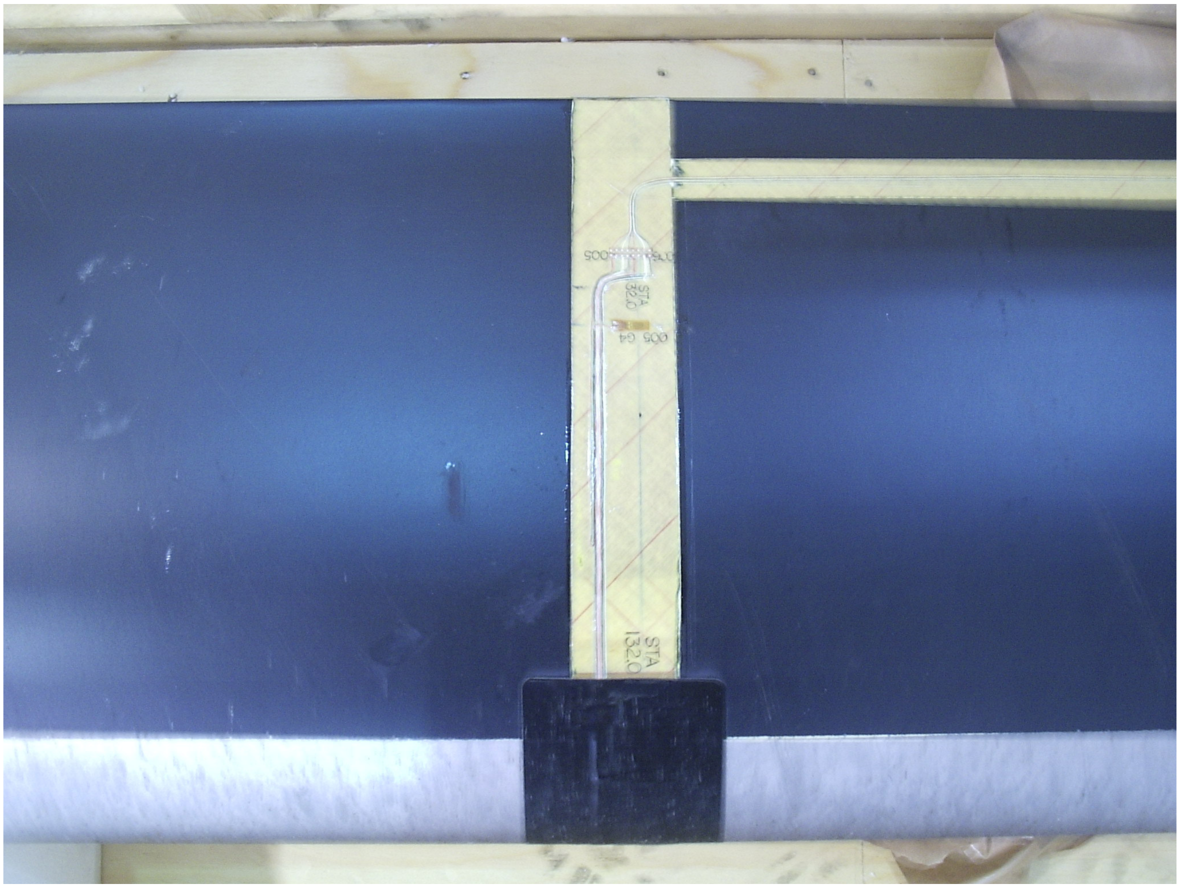

Figure 8: Instrumented Bell 412 main rotor blade gauges at station 132

3 TEST MATRIX

The test points flown involved steady state and dynamic conditions throughout the aircraft flight envelope. They consisted of hover, low speed regime, forward flight to VNE, climbs, descents, autorotative descents, coordinated turns up to 45 degrees of bank, steady heading side slips, step inputs, frequency sweeps, hover maneuvers and hovering in close proximity to a hangar. For the steady state test points, data collection was conducted for 30 seconds to 1 minute. Prior to measuring pressure data, a purge was performed, followed by a zero calibration of all the pressure transducers. This ensured that the pressure lines were clear of obstructions and a current offset value was stored for the system.

During the air wake tests, anemometers were placed around the aircraft to measure the air flow from the rotor. The anemometers were ultra-sonic, and provided airflow speed and direction in three dimensions. The anemometer placement consisted of various grids as shown in Figure 9, and testing was performed both in the presence of a hangar (designated H) and in a clear field (designated F) free of obstructions. After the testing, the anemometer locations were measured using a differential GPS set-up and averaged over a minute. This ensured accurate measurement of the anemometer placement. Additionally, free stream anemometers were located at the north-west corner of the hangar and at two other locations on the ramp well away from obstructions or the aircraft, and the locations of these were also determined. The anemometer tower located closest to the aircraft had 7 anemometers at varying heights, while the three other towers had a single anemometer located at the highest point, as shown in Figure 10. In the locations in Figure 9 where only one tower is indicated, the 7 anemometer tower was used.

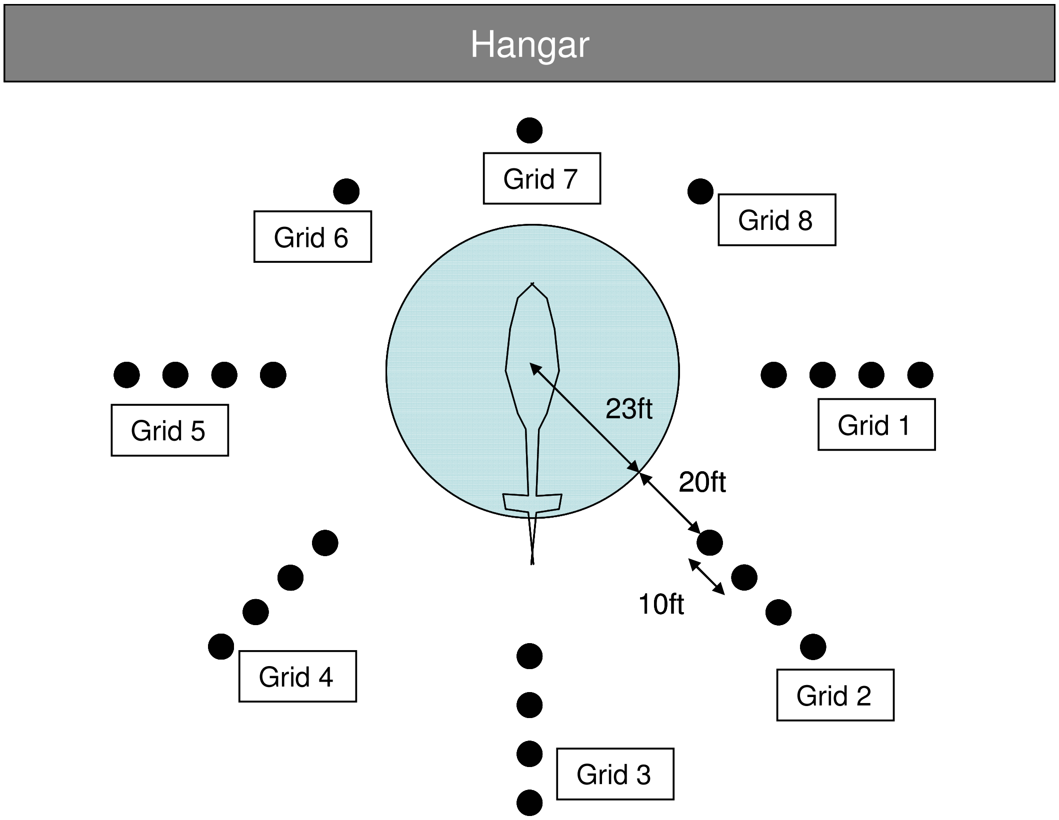

Figure 9: Hangar anemometer locations

Figure 10: Anemometer apparatus

4 DATA PROCESSING

The data collected included a variety of data streams at different rates. It was required to collate this into one coherent data set. This problem was compounded by the fact that the fuselage pressure data was collected in realtime at 62.5 Hz, however, it was transmitted to the data collection computer in one second bursts. The data recording format used on the aircraft is packet based with each packet containing a time stamp. The burst nature of the pressure data caused a severe time misalignment with all of the other data that was collected. This required the fuselage pressure data to be extracted separately from the raw data set and then recombined so that each data point would appear in the data stream at the correct point in time. The reference wind data signal was collected via a roof mounted anemometer and recorded on a separate ground-based computer. A GPS time stamp of this data was used to match the data with the aircraft data, which also included a GPS time stamp. The start and end time from each aircraft data file was extracted and used as indices to extract the wind data from each wind file. The 4 Hz wind data was then over sampled to match the data rate of the aircraft data. The air wake anemometer data was collected on a separate computer and was not linked with the aircraft data, however a GPS time stamp was collected to allow correlation between he two data sets.

Flap and lead-lag measurements were obtained using eight Hall effect sensors to measure the change in magnetic field caused by displacement of blade-mounted magnets. The voltage to displacement relationship for the flap sensor/magnet combination was known from a calibration performed on the previously used FRL rotor data telemetry system (Reference 3). A positive magnet displacement corresponded to an upward flapping motion of the blade. Zero displacement corresponded to the position of the blades when the rotor was not turning. The flap sensors and magnets were located on the damper bridge near the blade root. To convert a displacement measurement at the root to an equivalent blade tip flap angle, tip path measurements were collected using a laser-based rotor track and balance system. By comparison between the tip path measurements and the displacement measurements at the root, the system was calibrated. At the time of the flight test, the calibrations for flap, lead-lag, and strain had not been implemented in the real-time software of the rotor state measurement computer. This required the calibrations to be applied to the raw data after the flight testing was completed.

To relate a lag displacement at the blade root to a blade tip lag angle, it was assumed that blade bending in the lag direction is small and that a small angle approximation is valid, so the scale factor was determined from geometry.

The data collection flights were conducted before development of a real-time estimation algorithm in the rotor state computer was completed. Therefore, it was necessary to reconstruct azimuth, rotor RPM, and flap and lead-lag rotor states post-flight. Also, an intermittent connection inside the mast mounted data transmitter unit caused spikes in the flap and lead-lag data. These spikes were removed prior to rotor state estimation.

Azimuth and rotor RPM were measured by counting pulses from a 1 pulse-per-revolution sensor, as described in Reference 4. The main rotor azimuth angle is defined to be zero when the "red" blade (as identified by labels on the blades) is over the tail boom, and azimuth angle is positive in the direction of rotor rotation, i.e. counter-clockwise when viewed from above. The 1-per-rev sensor is triggered when the azimuth angle is 283°. The recorded data consists of a counter that increases with each revolution. To obtain rotor RPM, the counter data was converted to a series of one sample width pulses of amplitude $60 \cdot F_s$, where F_s is the sampling frequency of the rotor data (408 Hz). The pulses were then processed with a 2nd order Butterworth forward-reverse time filter with a break frequency of 0.5 Hz. A sample rotor RPM reconstruction is shown in Figure 11.

The azimuth angle ψ was reconstructed in a three step process. First rotor RPM was integrated to obtain azimuth with an unknown offset, ψ'. The correct offset ψ_0 was obtained by averaging the values of ψ' at the samples where the 1-per-rev sensor triggered, and then subtracting the average from 283°. Finally, the azimuth angle ψ was obtained by adding the offset ψ_0 to the integrated rotor RPM, ψ'.

Removal of the spikes from the flapping, lead-lag and strain data was nontrivial for several reasons. Firstly, most of the spikes were of very large amplitude, requiring a nonlinear filter that could selectively identify and remove the spikes without affecting the remaining data. Secondly, many spikes lasted longer than one sample, making it necessary to identify the beginning and end of each spike. Thirdly, spikes often occurred in bursts, with as little as one good data point between spikes. Due to the volume of data collected in this flight test program, it was not possible to manually correct each spike. As such, an automated process was developed to correct all of the data files. The result of this process is shown in Figure 12.

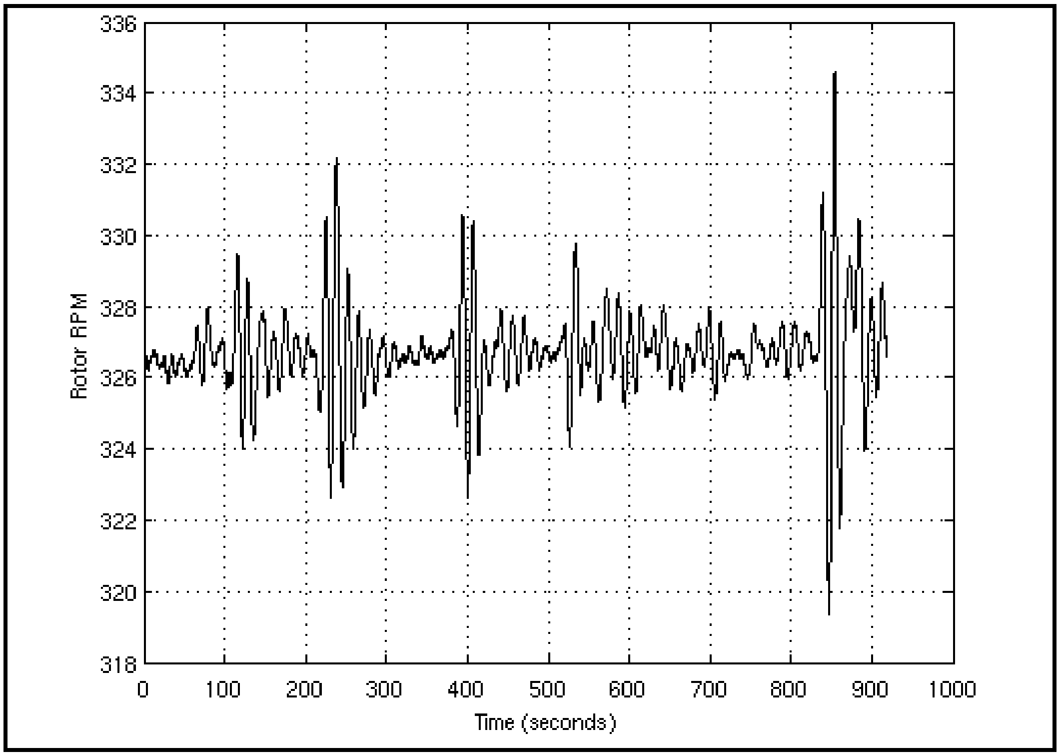

Figure 11: Reconstructed rotor RPM data.

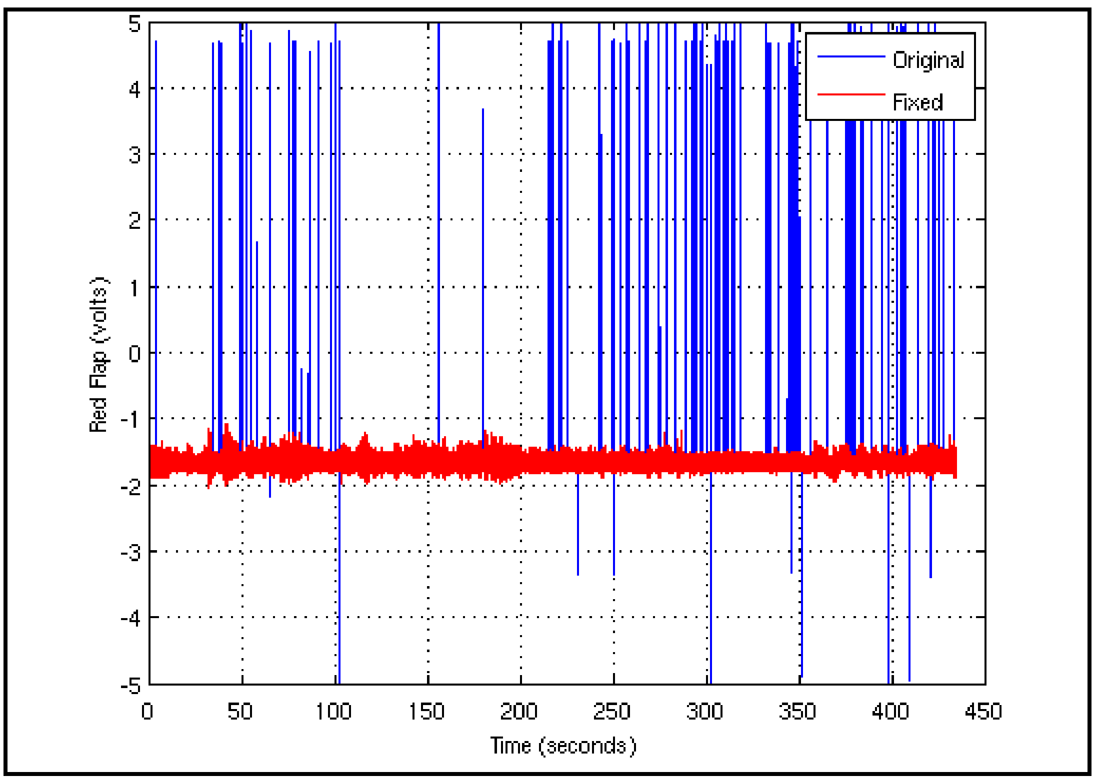

Figure 12: Example flap data time history with spikes removed.

The individual blade measurements of flap angle and lead-lag were converted into rotor states (coning, lateral and longitudinal tilt, global lead-lag, lateral and longitudinal lead-lag) via a time varying transformation and Kalman filter described in Reference 5. The continuous time equations from Reference 5 were converted to a discrete time estimator, as described in Reference 4. The resultant equations were applied to the data after the calibration coefficients had been applied and the spikes were removed.

5 FLIGHT TEST RESULTS

During the flight test program, large quantities of data were collected. Comprehensive analysis of this data has not been performed; however a selection of the pressure data is presented in this section of the paper. This data was selected to highlight interesting aspects of the flow field around a Bell 412 helicopter.

Airwake – general. A selection of the land-based anemometer data is plotted in Figure 13 to Figure 17. Figure 13 to Figure 16 compare velocity vectors with and without the presence of the hangar (red and green vectors respectively), while Figure 17 compares vectors at identical anemometer locations in the presence of the hangar but at two different wind conditions. In general, downwash predominates at the higher anemometers while outwash predominates at the lower anemometers where the flow is obstructed by the ground. As the aircraft ascends, outwash increases at the higher anemometers and decreases at the lower anemometers. On the starboard side (right when looking from behind) of the aircraft, the flow tends to flow down and out, whereas on the port side (left when looking from behind), a rotating flow is visible, with inwash at the highest anemometers and outwash at the lowest. Potential causes for the asymmetry include the ambient wind, the effect of the tail rotor, and the swirl component of the flow.

Hangar effect. Figure 13 shows data for anemometers placed on either side of the aircraft, as described in the top right corner of the plot, and includes cases for rotor heights from 12 feet (aircraft light on skids) to 32 feet (skids 20 feet above ground level). Figure 14 shows the same anemometer locations with rotor heights from 42 feet (30 feet AGL) to 112 feet (100 feet AGL). The ambient winds conditions for Figure 13 and Figure 14 are indicated in the top right corner of the plot. Figure 15 and Figure 16 present data in a similar manner to Figure 13 and Figure 14, except that the anemometers were placed in front and behind the helicopter in this case. The effect of the hangar on the flow field at Grid 1H/F is shown in Figure 13 and Figure 14. At these anemometer locations, the downwash is significantly increased in the presence of the hangar, although it is possible that the change in downwash is also influenced by the ambient wind. The hangar has a much smaller effect at the anemometer locations aft of the helicopter (Grid 3H, Figure 15 and Figure 16). At Grid 7H (Figure 15 and Figure 16, left side), only upwash is measured at the anemometers, except when the rotor is at 112ft. Here the rotor downwash is confined to the area between the aircraft and the hangar, and is forced upward by the hangar face. It is likely that some of this upwash is re-ingested by the rotor, but this is not evident in the plots.

Ambient wind effect (in the presence of the hangar). Figure 17 shows the data for two different wind conditions for anemometers placed on the starboard aft side of the aircraft (135 degree relative bearing from the front), and includes cases for rotor heights from 12 feet (aircraft light on skids) to 112 feet (100 feet AGL). The ambient winds conditions for Figure 17 are indicated in the top left corner of the plot. Data measured on the first day, when winds were generally light and from 180° relative to the helicopter heading, are colored green. Data measured on the second day, when winds were stronger and from 315° relative to the helicopter, are colored red. The ambient wind appears to have a strong effect on the flow field as the wind skews the rotor downwash onto or away from the anemometers. The flow field is particularly affected at the upper anemometers located at 20 feet for rotor heights between 12 and 52 feet, with the effect of the ambient wind diminishing more quickly at lower anemometer heights. Of particular interest is the evidence of inwash at the lowest anemometers when the rotor is at 102 feet, indicating the possible formation of a contra-rotating vortex directly beneath the rotor.

Surface pressure – Straight and level. The data for Figure 18 was collected while in straight and level flight at an average pressure altitude of 3000 feet and at true airspeeds between 32 and 128 knots. The data at each stabilized speed was collected for a period of 60 seconds and averaged to provide surface pressures around the aircraft fuselage. As the airspeed increases a strong impingement of flow is seen developing on the nose and forward edge of the transmission cowling of the aircraft with a slightly smaller impingement of flow on the upper side of the horizontal stabilizer. Of note is the area behind the main fuselage (where the fuselage narrows and the tailboom attaches to the main fuselage), which shows surface pressures very close to ambient regardless of forward speed indicating very little air flow. As airspeed increases, a strong acceleration of flow can be seen at the top end of the pilot window (just as it rounds the corner with the top of the fuselage), on the top side of the transmission cowling, at the engine inlet and on the bottom side of the horizontal stabilizer. The vertical stabilizer, sides and bottom of the fuselage also show signs of slight flow acceleration as airspeed increases.

Surface pressure – Low speed. The data for Figure 19 was collected while flying at low speed in light wind conditions and at a skid height of 35 feet (high enough to be mostly out of ground effect while low enough to have good visual references to maintain a constant speed). The data at each stabilized speed was collected for a period of 30 seconds and averaged to provide surface pressures around the aircraft fuselage at a relative flight direction of 240 degrees (wind from the left aft quarter when viewed from above). The top diagram (0 knot hover) shows evidence of a slight asymmetry in the flow just ahead of the horizontal stabilizer, indicating the possible location of the main rotor downwash striking the tailboom. Accelerated flow can also be seen at the nose of the aircraft, while a strong impingement of flow is evident on the right hand side of the vertical stabilizer due to the presence of the tractor tail rotor. As the relative speed increases to 15 knots, the vertical stabilizer impingement reaches its peak possibly indicating an interaction between the tail rotor and the relative wind. Furthermore, as the speed increases, a strong asymmetry of flow is present on the left side of the main fuselage and tailboom, with the left side indicating a deceleration of flow. The exception to this is on the left underside of the aircraft at 35 knots of relative wind, which show signs of flow acceleration. Of note is the strong impingement of flow slightly ahead of the main transmission at 15 knots, possibly indicating an interaction between the main rotor flow and relative wind. The engine inlet surface pressure also indicates flow acceleration with a slight asymmetry at relative speeds greater then 10 knots.

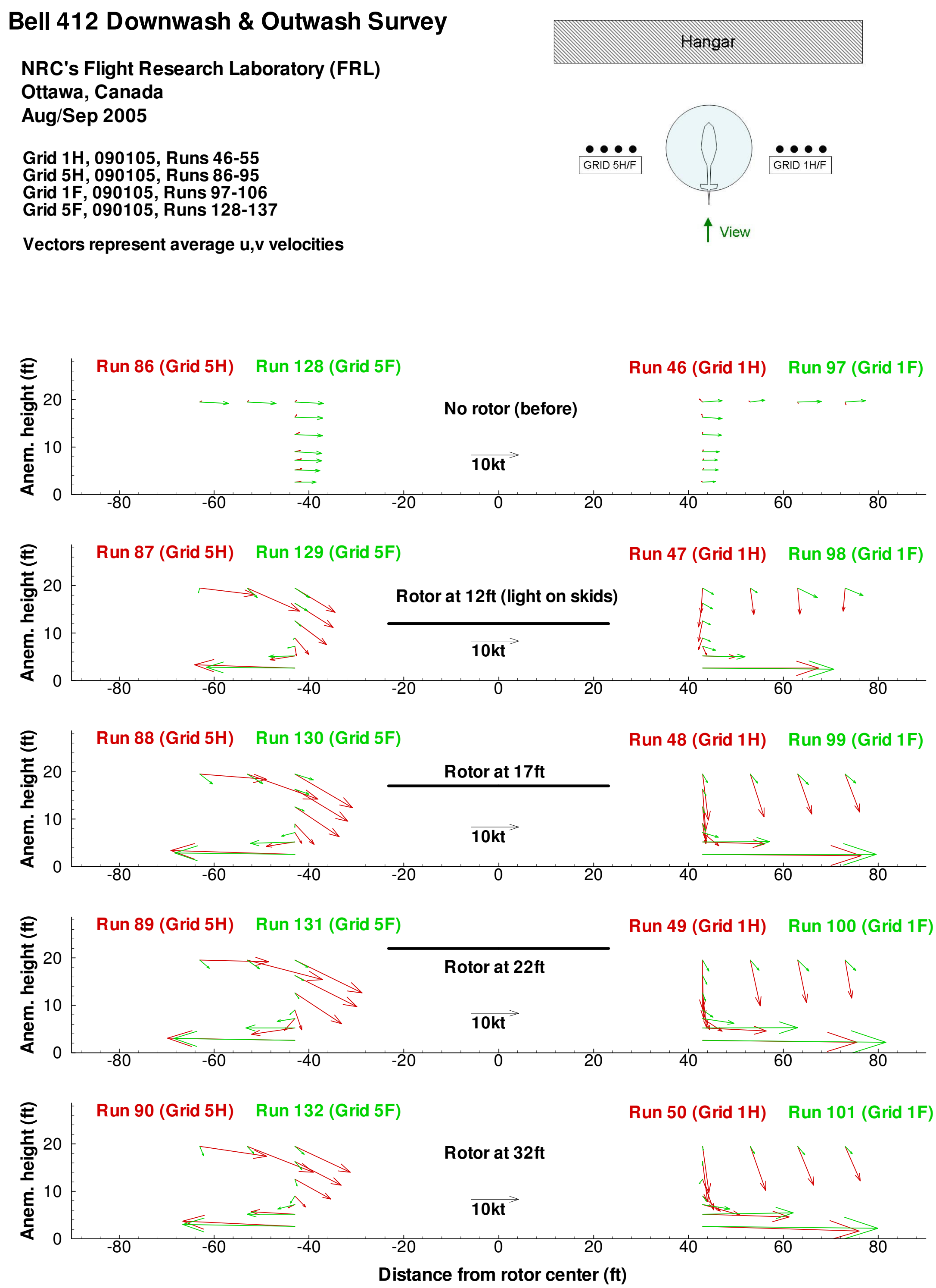

Figure 13: Velocity Vectors at Grids 1H, 5H, 1F and 5F – Red in presence of hangar, Green without

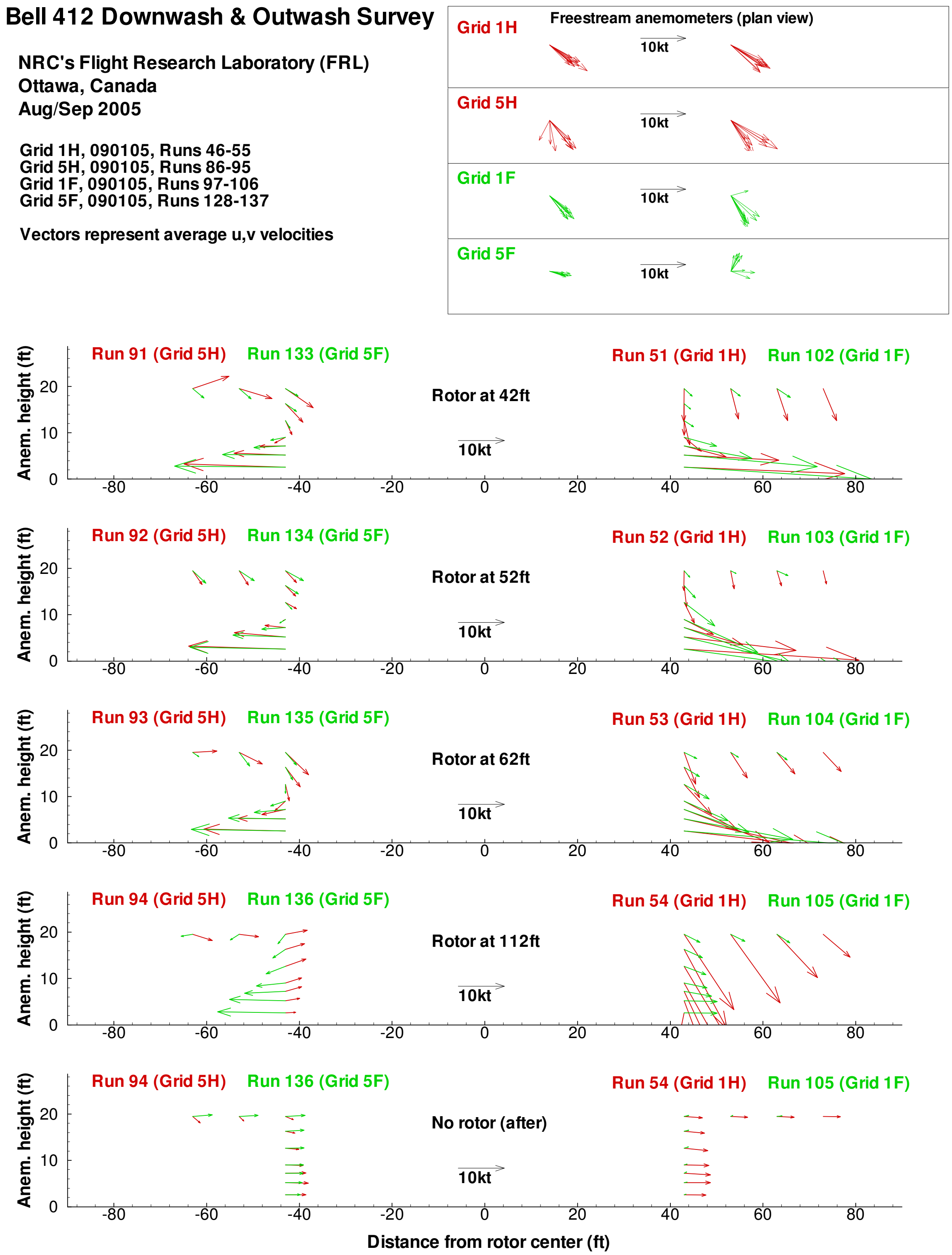

Figure 14: Velocity Vectors at Grids 1H, 5H, 1F and 5F – Red in presence of hangar, Green without

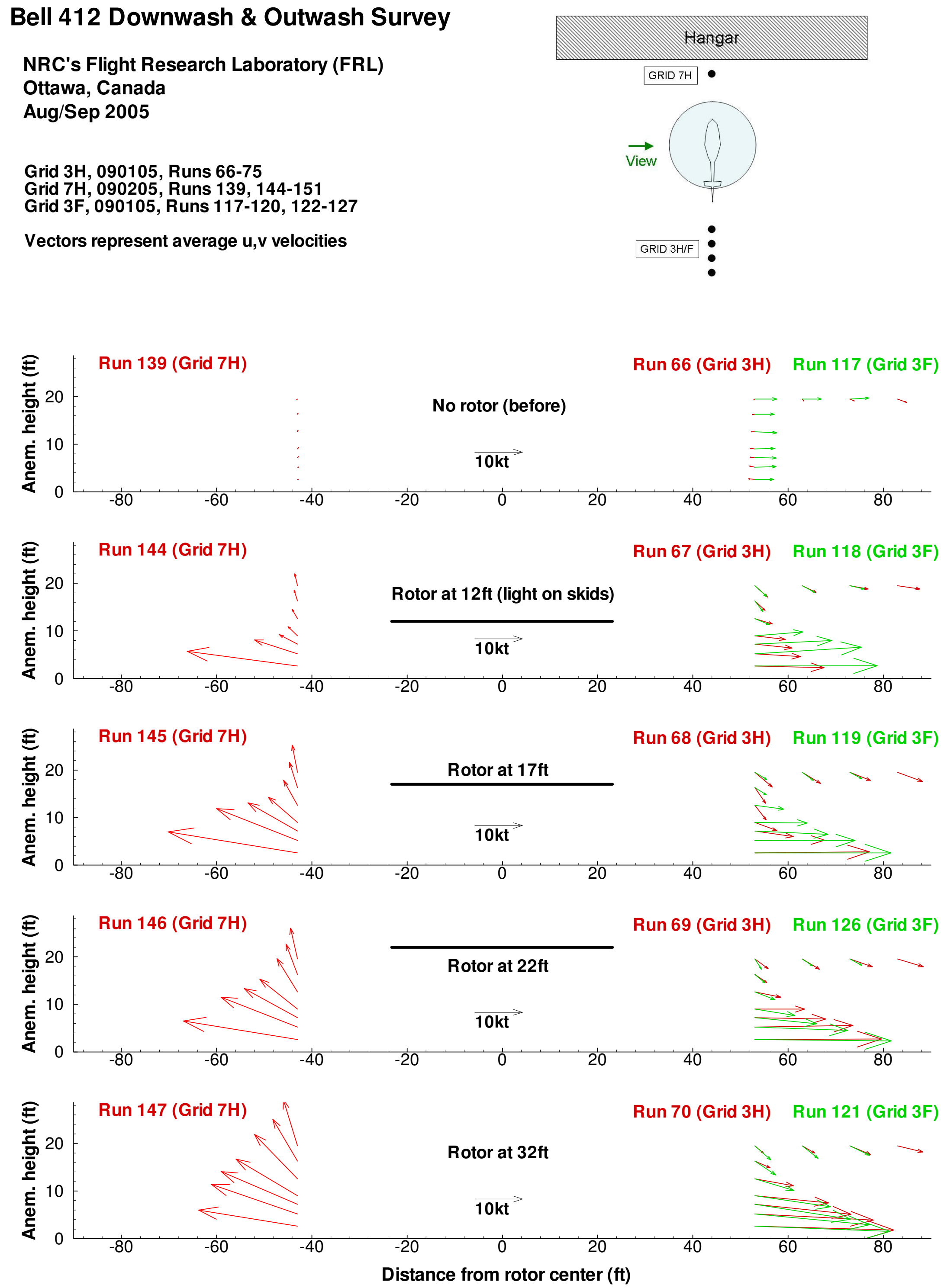

Figure 15: Velocity Vectors at Grids 3H, 7H and 3F – Red in presence of hangar, Green without

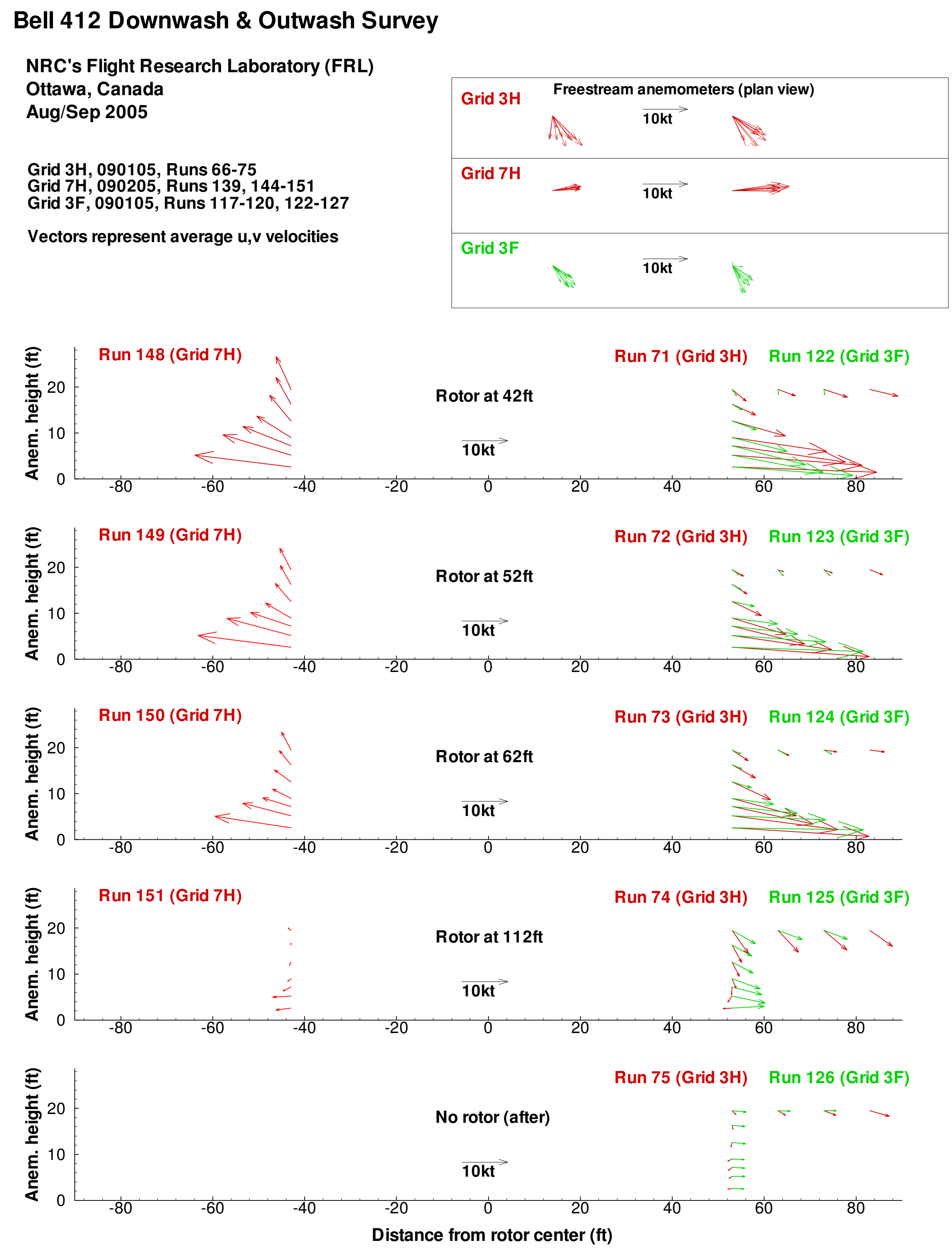

Figure 16: Velocity Vectors at Grids 3H, 7H and 3F – Red in presence of hangar, Green without

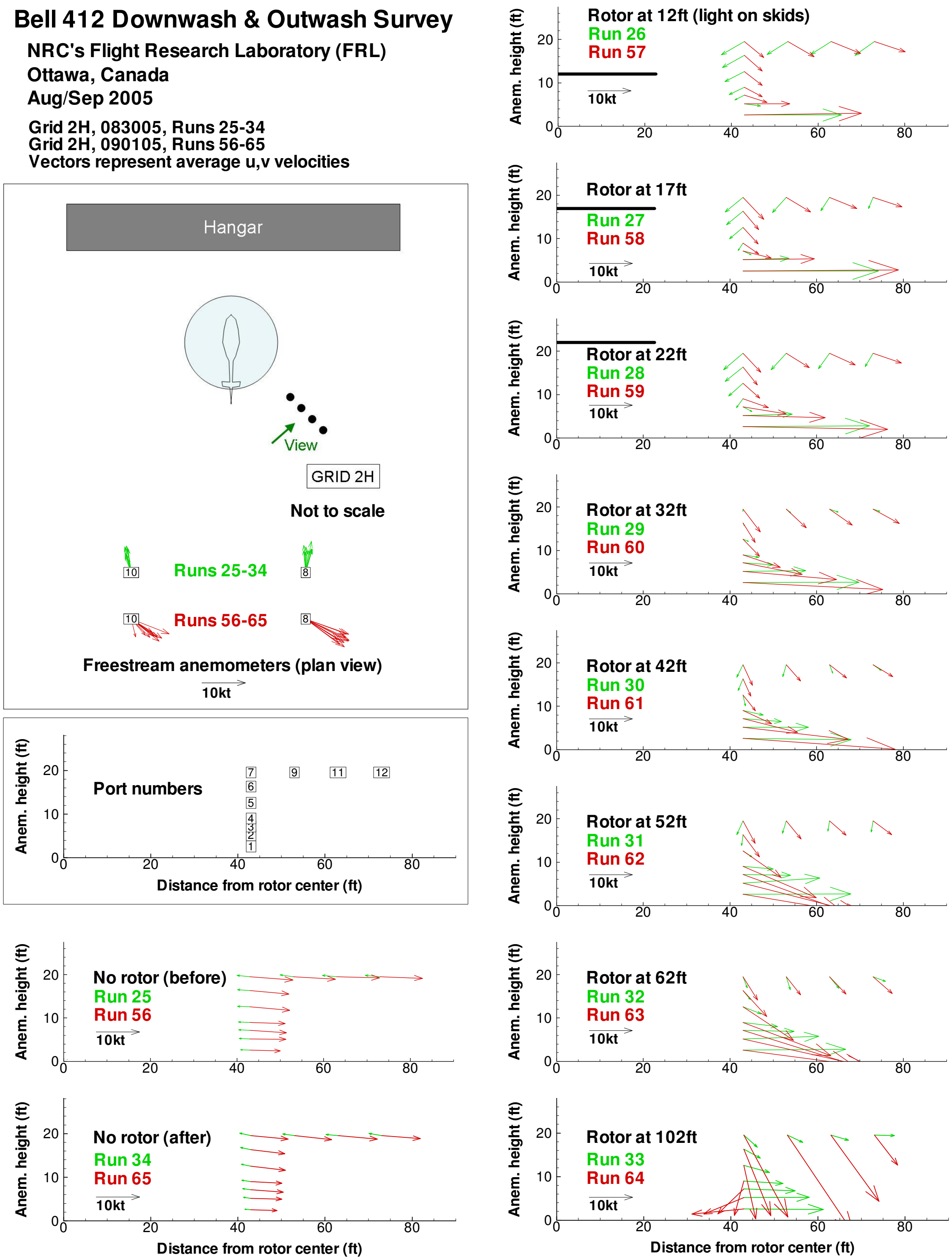

Figure 17: Effect of Ambient Wind at Grid 2H – Green represents light winds, Red higher winds

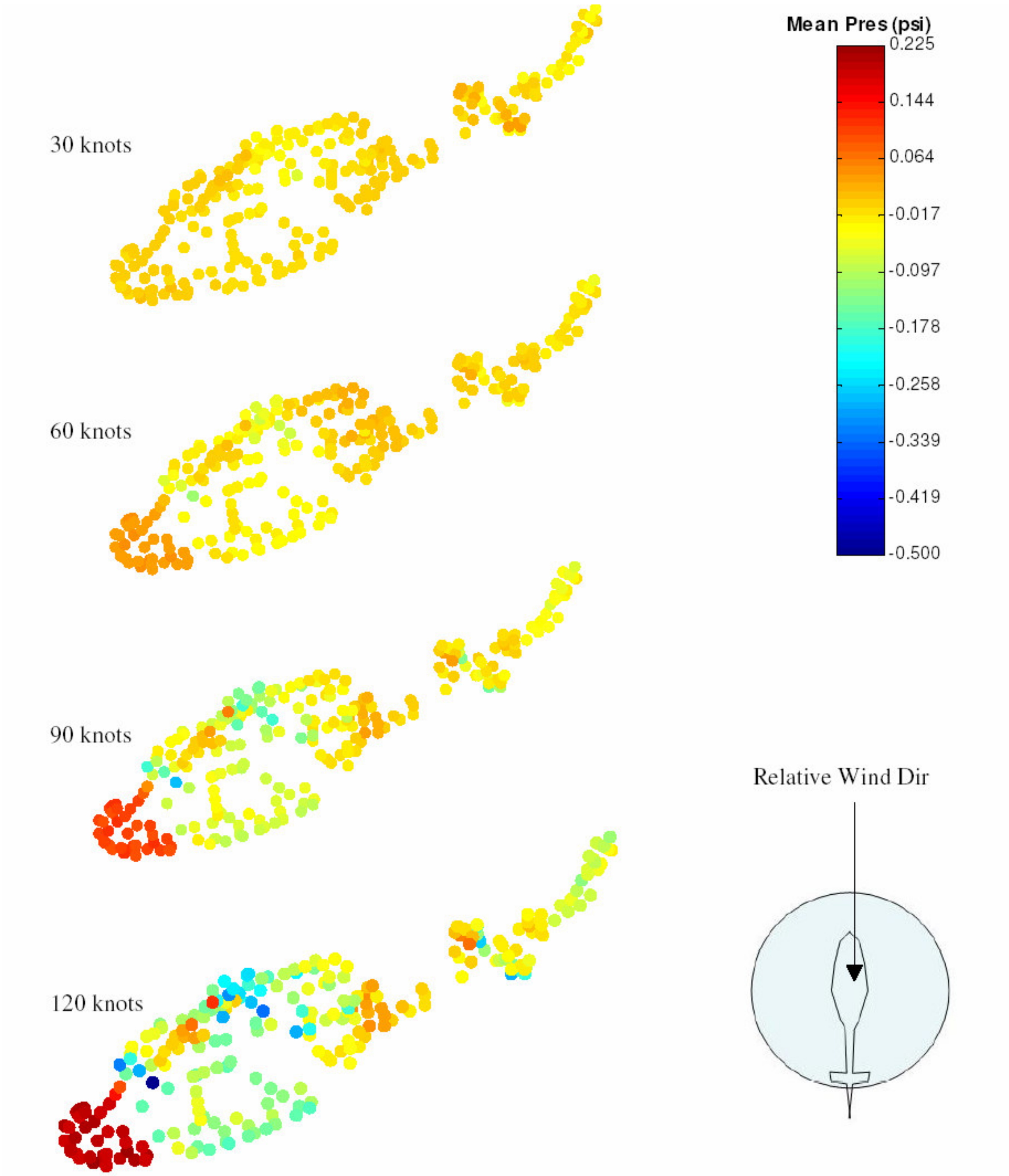

Figure 18: Average fuselage pressures at various airspeeds and 3000 ft altitude

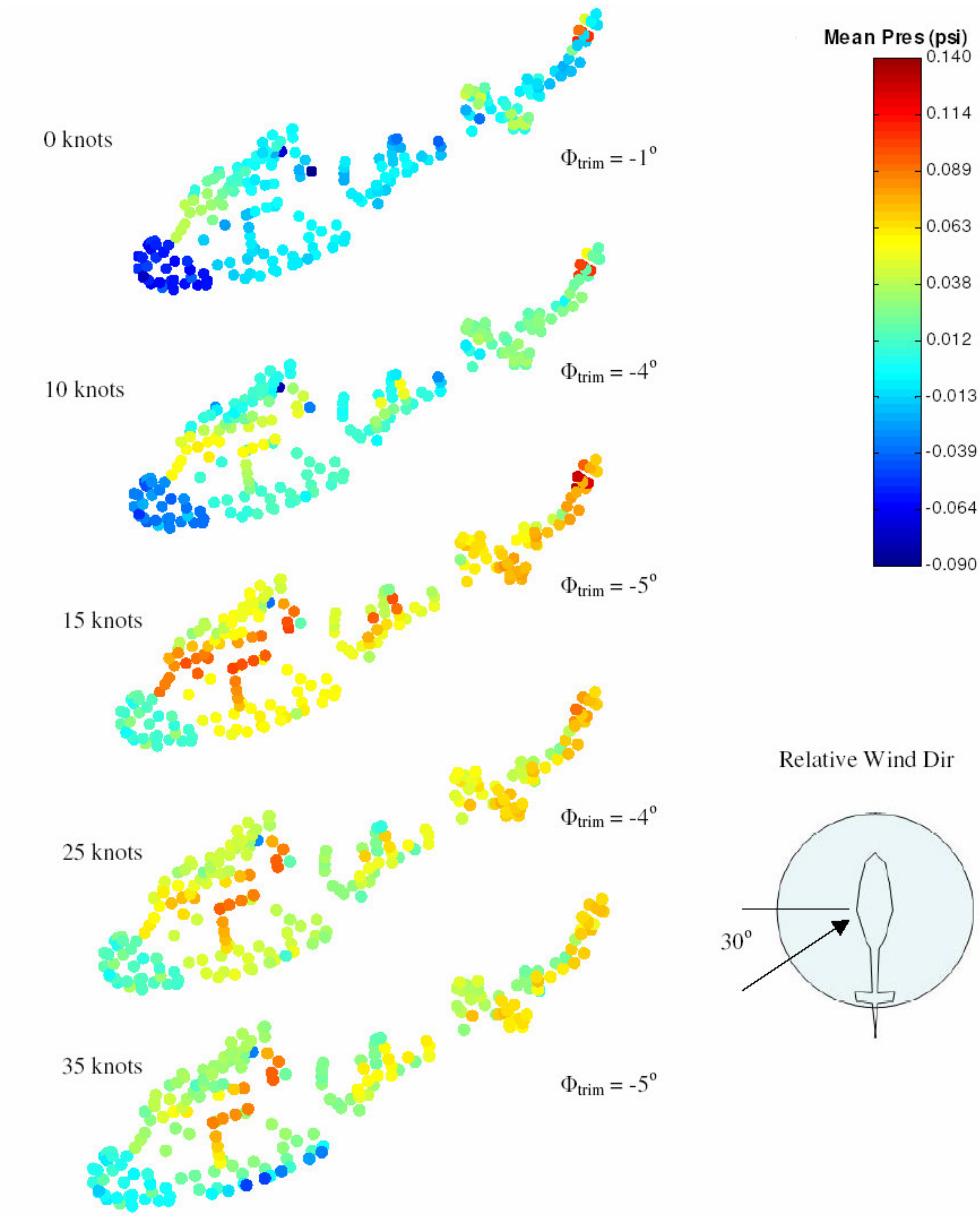

Figure 19: Average fuselage pressures at various windspeeds for a relative wind direction of 240 degrees

6 SUMMARY

This paper described a flight test program conducted by the National Research Council of Canada Flight Research Laboratory on a Bell 412 helicopter. The aircraft was instrumented with a fuselage pressure measurement system to determine surface pressures around the aircraft in flight. Ground based anemometers were used to collect air wake data. The purpose of the flight test was to acquire fuselage pressure data in various flight regimes and air wake data in the hover, both in front of a hangar and in free air. This data is suitable for future full scale validation of CFD models and will increase the understanding of the complex flow around a helicopter in flight.

7 ACKNOWLEDGEMENTS

The authors would like to thank Bell Helicopter Textron Canada (BHTC), in particular Bogdon Mijatovic, for aiding with information regarding the strain gauging of the Bell 412 rotor blades. Many thanks as well to the Aerospace Engineering Test Establishment (AETE) of the Canadian Department of National Defense for the loan of the instrumented Bell 412 main rotor blade. This work was partially funded by the US Naval Air Systems Command and the Canadian Department of National Defense.

8 REFERENCES

[1] Gubbels, A.W., Ellis, D.K., "NRC Bell 412 ASRA FBW Systems Description in ATA 100 Format", National Research Council of Canada, Institute for Aerospace Research, Laboratory Technical Report, LTR-FR-163, April 2000.

[2] Dillon, J., "Real-time Implementation of a Strapdown Inertial/GPS Integrated Navigation System", National Research Council of Canada, Institute for Aerospace Research, Laboratory Technical Report, LTR-FR-213, October 2004.

[3] Alexander, M., Gubbels, A.W., Dillon, J., "Development of a Rotor State Measurement System for the NRC Bell 412 Advanced Systems Research Aircraft", Proceedings of the 59th American Helicopter Society Annual Forum, Phoenix AZ, May 6-8, 2003.

[4] Dillon, J., Ellis, K., "Development of a Rotor State Measurement System for the NRC Bell 205 Airborne Simulator", LTR-FR-232, May 2005.

[5] Fuller, J. W., "Rotor State Estimation for Rotorcraft", American Helicopter Society, November 1981.